Supplementary Article:

S1. Processing optimization

S1.1Calcination

To estimate the calcination temperature, thermogravimetric analysis is used (Fig.S1(a)). The TGA analysis performed up to 1000 ºC revealed the weight loss after 840 ˚C, which infers the formation of the (SmSr)$NiO_{4-\delta}$ compound after 840 ºC. In addition, a kink is also observed at 278 ºC, indicating removal of CO instead of CO_2 as depicted through weight loss percentage according to the following reaction:

$$Sm_2O_3 + 2SrCO_3 + 2NiO \rightarrow 2(SmSr)NiO_{4-\delta} + 2CO + \frac{1+\delta}{2}O_2$$

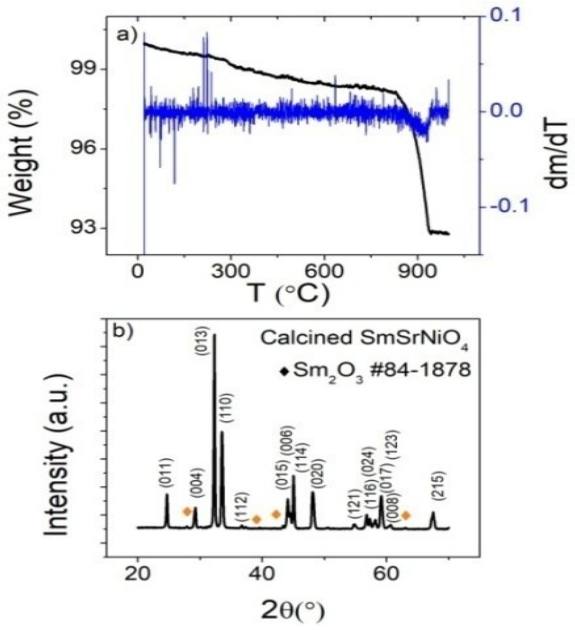

Fig.S1 (a) TGA, DTGA of raw powder and (b) XRD of calcined powder (SmSr)$NiO_{4-\delta}$

Further, differential thermal analysis is also showing a disturbance around 280 ºC and a kink at 840 ºC, but after that again, an increase is observed. This rise further corresponds to the oxidation of the samples. Hence, the calcination should be done well above 1000 ºC for the proper oxygen

content, according to the Ruddlesden Popper phase. Fig.S1(b) depicts the X-ray diffractogram of the powder calcined at 1200 ^{o}C for 3hr and matches well with the tetragonal phase (I4/mmm symmetry) according to JCPDS File No. 480973. The XRD pattern of the calcined powder is refined using Full Prof Suite package with I4/mmm symmetry. The refinement is done using peak profile Thomson Cox Hastings Pseudo Voigt and Axial divergence symmetry along with the instrument parameters, and the refinement factors obtained are R_f = 3.66 and Bragg R-factor = 5.66. The lattice parameters obtained are a = b = 3.7786 Å and c =12.2289 Å.

S1.2 Sintering

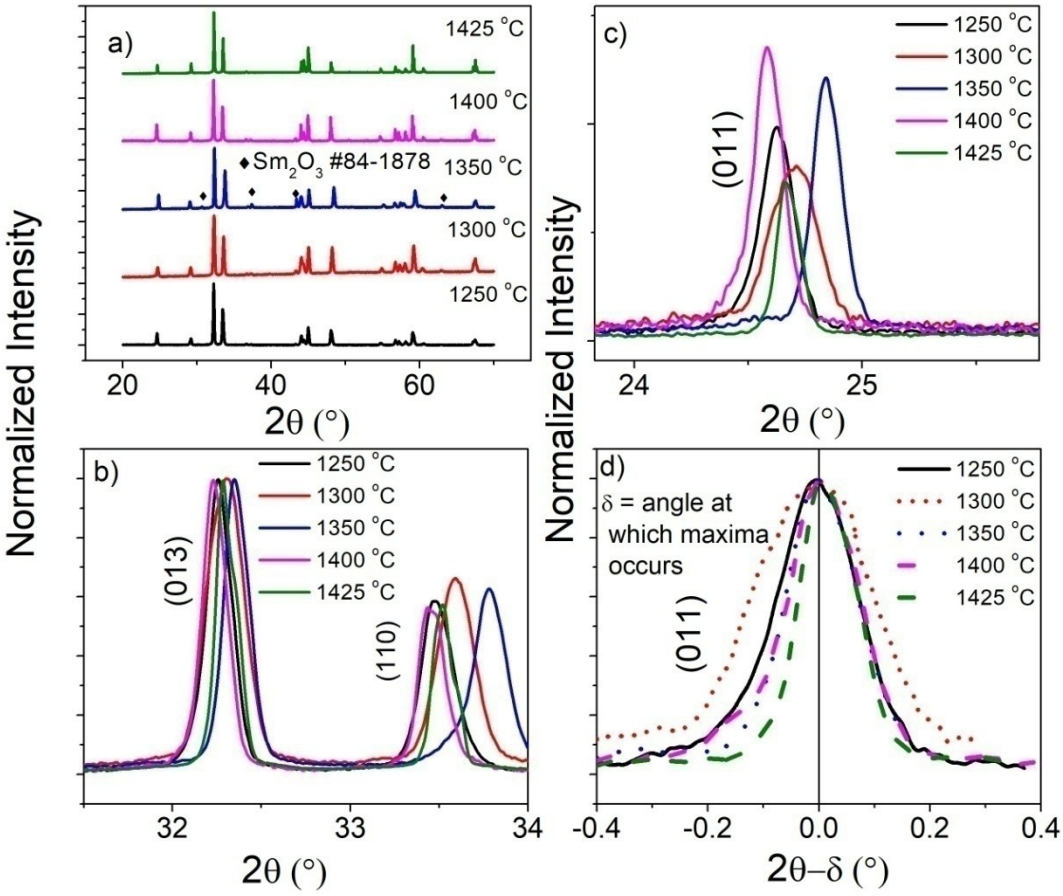

Fig.S2 (a) XRD pattern of the (SmSr)$NiO_{4-\delta}$ sample sintered at different sintering temperatures 1250 ^{o}C, 1300 ^{o}C, 1350 ^{o}C, 1400 ^{o}C and 1425 ^{o}C, (b) Shifting and FWHM of the studied samples corresponding to 2θ ~ 32^{o}, (c) Shifting and FWHM of the studied samples corresponding to 2θ ~ 24^{o}, (d) Diffuseness of XRD peak (011) corresponding to 2θ ~ 24^{o}

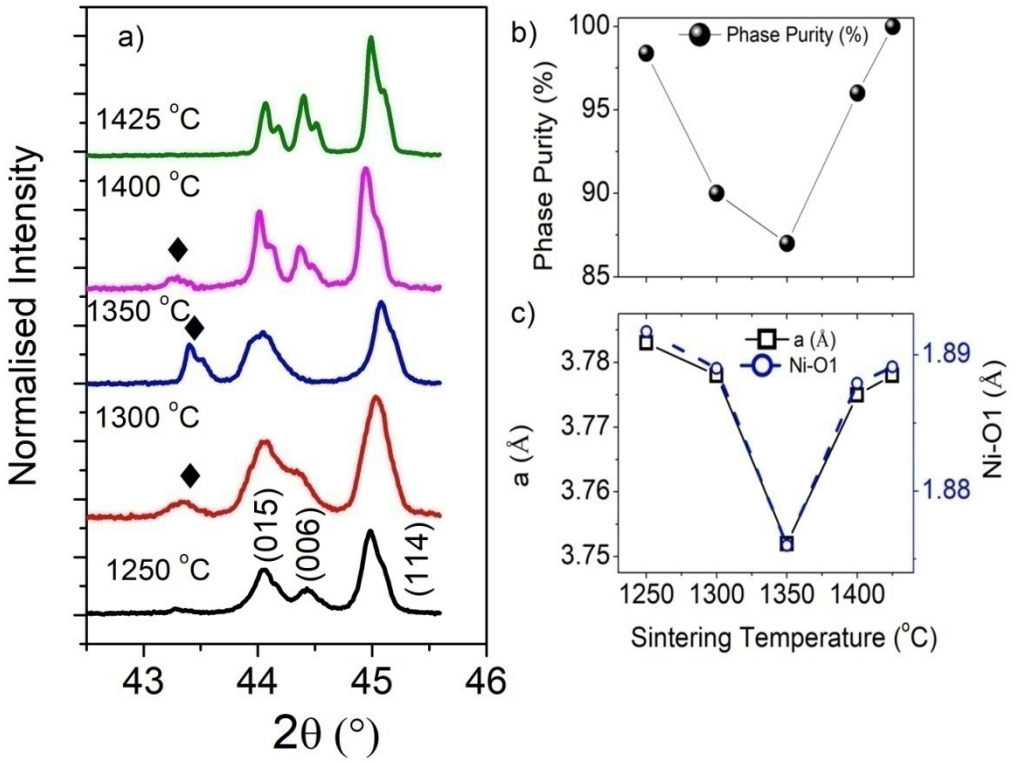

Fig.S3 (a) X-ray diffractograms of the (SmSr)$NiO_{4-\delta}$ sample sintered at different sintering temperatures 1250 ^oC, 1300 ^oC, 1350 ^oC, 1400 ^oC and 1425 ^oC corresponding to $2\theta \sim 43^o$ - 46^o, (b) Phase purity of the studied samples (c) Variation of lattice parameters and Ni-O1 distance with the sintering temperature.

After the nearly single phase formation of calcined powder as confirmed through Rietveld refinement, the sintering temperature is varied, and the sample is sintered at 1250 ^oC, 1300 ^oC, 1350 ^oC, 1400 ^oC, and 1425 ^oC to get clean phase.

The XRD of (SmSr)$NiO_{4-\delta}$ sample sintered at different temperatures reveal the single phase of the samples (Fig.S2(a)). The secondary phases are observed to occur in the sample sintered at 1350 ^oC belonging to Sm_2O_3 (JCPDS File No. 84-1878). Fig.S2(b) and (c) correspond to the peaks (013), (110), and (011) at $2\theta \sim 32^o$, 33^o and 24^o, respectively. It can be seen that there is uniform FWHM for (013) peak instead of (110) and (001) peak. To observe this shifting keenly, diffuseness has been plotted using (011) peak. Fig. S2(d) shows the variation of Intensity with 2θ-δ, where δ is the angle where maxima occur. It can be seen that before 1350 ^oC, the XRD peaks diffuse towards lower angle while for sintering temperature greater than 1350 ^oC, XRD peaks diffuse towards higher angle. The XRD peaks observed here are also seen to possess angle shifting with the sintering and hence, lattice parameter alteration.

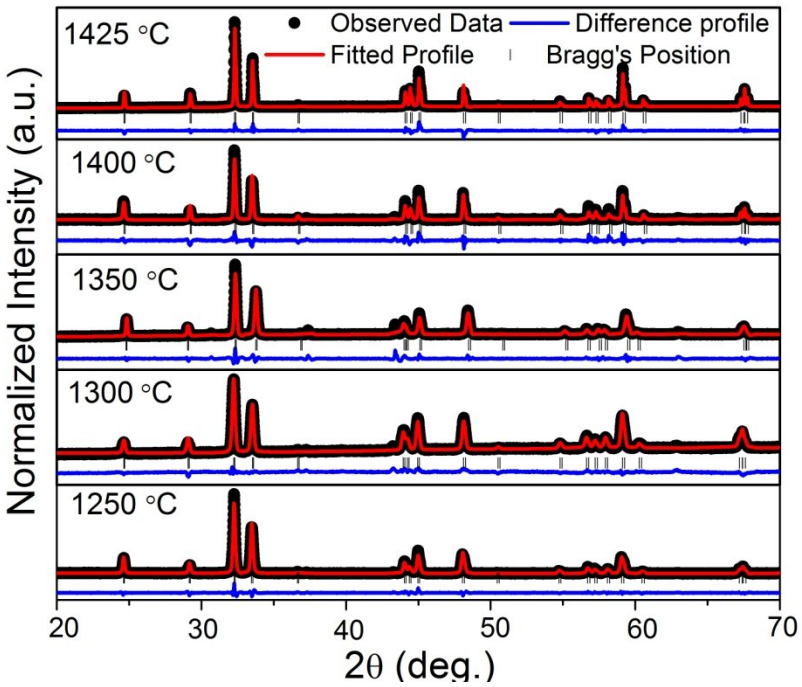

Fig.S4 Rietveld refined X-ray diffractograms of the (SmSr)$NiO_{4-\delta}$ sample sintered at different sintering temperatures 1250 °C, 1300 °C, 1350 °C, 1400 °C, and 1425 °C. The figure contains the data points, intensity obtained, difference profiles and Bragg positions of the samples sintered at different temperatures.

A careful analysis regarding the secondary phase is shown in Fig.S3(a). The intensity of the secondary phases observed in the calcined powder decreases with the sintering at 1250 °C, further observed to increase with the increase in sintering temperature up to 1350 °C and then decreases again with the further rise in sintering temperature. Hence, the phase purity of all the samples is determined using $\varphi_{purity} = \frac{I_p}{I_p + 0.8\, I_s}$, I_p is the maximum intensity of primary peak and I_S is the maximum intensity of the secondary phase. Fig.S3(b) shows that the phase purity is minimum for the sample sintered at 1350 °C and maximum at 1425 °C (~100%). For further clarifications regarding the phase purity, XRD patterns have been refined with I4/mmm symmetry and peak profile Thomson Cox Hastings Pseudo Voigt and Axial divergence symmetry. The lattice parameter and Ni-O1 bond distance obtained thereof from refinement are plotted in Fig.S 3(c). It is observed that a and Ni-O1 bond distance are observed to decrease up to 1350 °C, and then after that increases with the increase in sintering temperature. The Rietveld refined XRD is shown in

Fig. S4 and the refinement factors lie within the appreciable error range. The atomic positions, occupancy, and R-factors are listed in the TableS1 for the ready reference. From structural results, it can be seen that the sample sintered at 1350 ^{o}C is highly impure.

Table S1 Atomic positions and R-factors obtained after refinement for the (SmSr)$NiO_{4-\delta}$ samples sintered at different temperature

Sample	Sintering Temperature (^{o}C)	Atoms	Position coordinates			Occupancy	R-factors	
			x	y	z		Bragg R-factor	R_f factor
T1	1250	Sm	0	0	0.3611(7)	1.02417	3.27	2.11
		Sr	0	0	0.3611(7)	0.99593		
		Ni	0	0	0	1.01461		
		O1	0	0.5	0	1.07190		
		O2	0	0	0.1639(7)	1.31416		
T2	1300	Sm	0	0	0.3636(5)	0.92552	13.4	9.73
		Sr	0	0	0.3636(5)	1.08606		
		Ni	0	0	0	1.10007		
		O1	0	0.5	0	1.28083		
		O2	0	0	0.1642(0)	1.00506		
T3	1350	Sm	0	0	0.2448(8)	0.79725	4.98	4.09
		Sr	0	0	0.2448(8)	1.31250		
		Ni	0	0	0	1.02844		
		O1	0	0.5	0	1.24411		
		O2	0	0	0.1691(4)	1.05810		
T4	1400	Sm	0	0	0.3617(7)	0.97339	9.81	5.78
		Sr	0	0	0.3617(7)	0.90265		
		Ni	0	0	0	1.04320		
		O1	0	0.5	0	1.01023		
		O2	0	0	0.1653(0)	1.12311		
T4	1425	Sm	0	0	0.3615(1)	0.88110	6.15	4.04
		Sr	0	0	0.3615(1)	1.07557		
		Ni	0	0	0	1.30212		
		O1	0	0.5	0	0.99270		
		O2	0	0	0.1608(3)	1.03581		

S2 Microstructural Studies and Density

As Density being an important parameter not only for the optimization of the sintering temperature but also for a primary requisite for the cathode and electrolyte materials for SOFC. The density is observed to increase with the increase in sintering temperature up to 1400 ^{o}C and then reduces after that at 1425 ^{o}C, as shown in Fig. S5.

For the morphology, densification and grain growth, FESEM micrographs are studied for the (SmSr)$NiO_{4-\delta}$ sample sintered at different sintering temperatures (Fig.S6(a-e)). The sample sintered at 1250 ^{o}C is showing well connected, porous, and well-developed grains, as seen through the formation of water-marks on the surface of grains. In addition, grain size is observed to increase with the increase in sintering temperature and is observed as 1.236 μm, 2.659 μm, 2.748 μm and 4.129 μm for the samples sintered at 1250 ^{o}C, 1300 ^{o}C, 1350 ^{o}C, and 1400 ^{o}C, respectively. The increase in grain size is leading to a reduction in porosity with the increase in sintering temperature. Whereas, the long channel formation on the surface of grains is seen in the sample sintered at 1425 ^{o}C (Fig.S6(e)) as the grains have enlargened enormously (Fig.S6(e) inset). This is showing the change in surface behavior of the sample sintered at 1425 ^{o}C in comparison to 1250 ^{o}C. Further, EDX has been studied and showing that at 1400 ^{o}C, the sample is highly Ni-rich and O deficient (Fig.S6(f)). Thus, surface behavior has altered due to Ni and O alteration.

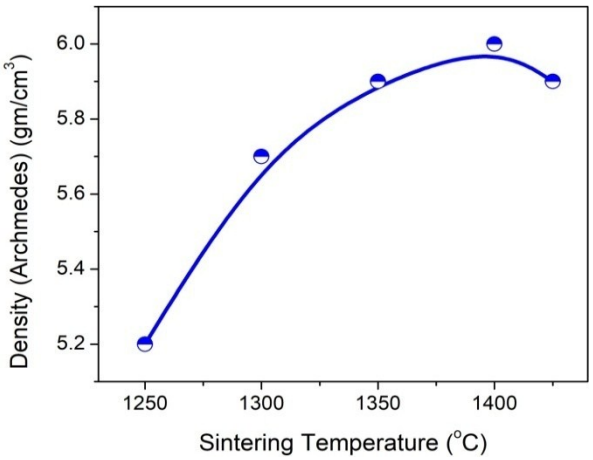

Figure S5 Variation of density with the increase in sintering temperature showing a hump at 1400 ^{o}C, proving the optimized sintering temperature.

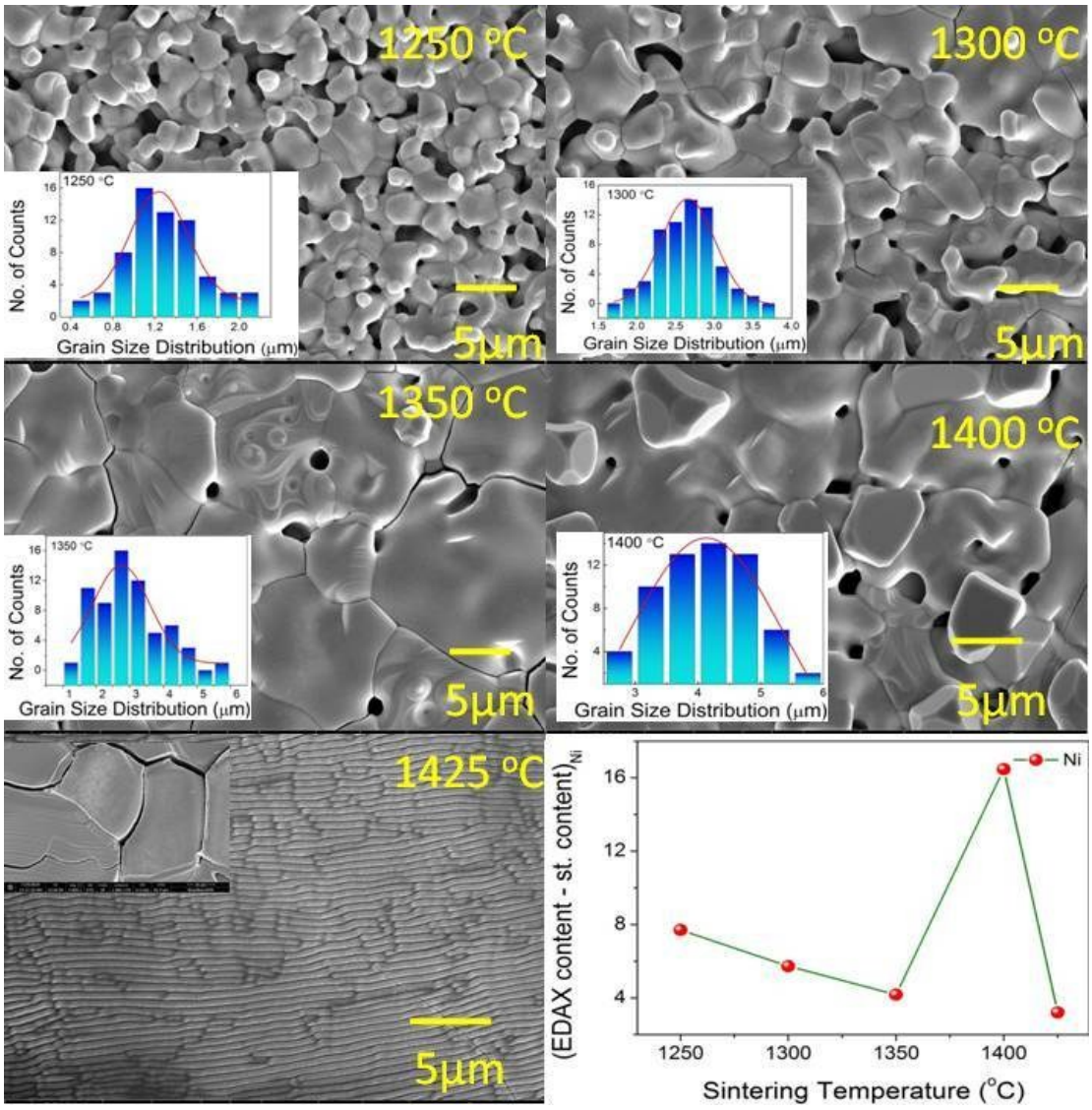

Figure S6(a-e) SEM micrographs of (SmSr)NiO_{4-d} sample sintered at different sintering temperatures (e) inset surface of the sample sintered at 1425 °C and (f) Excess Ni measured through EDX of the studied samples.

S3. FTIR studies

The different oxides band formations and hydroxyl band groups, are studied through the FTIR transmission spectra of all the samples sintered at different sintering temperatures (Fig.S7(a)). The absorption band at 400 cm^{-1} and range 527-581 cm^{-1} correspond to Ni-O bond. Fig. S7 (b) shows the zoomed part of FTIR spectra in the wavenumber range of 400-700 cm^{-1}. It

is observed here that 400 cm^{-1} and 527 cm^{-1} modes are complimentary that the intensity corresponding to 400 cm^{-1} increases while intensity corresponding to 527 cm^{-1} mode decreases. The band at 1000 - 1250 cm^{-1} corresponds to Sm^{3+}-O-Sm^{3+} asymmetric stretching. Moreover, with the increase in sintering temperature, the peak positions corresponding to Sm^{3+}-O and Ni-O are observed to vary, showing the changes in electronic structure due to electronic effects. The bands corresponding to H-O-H observed in the range of 2700 - 4000 cm^{-1}, O-H band corresponding to 1601 - 1615 cm^{-1} are not shifting with the sintering temperature. Rather, their intensities are observed to vary with the increase in sintering temperature. In addition, the intensity of Ni-O band at 400 cm^{-1} is lower in the sample sintered at 1425 ^{o}C in comparison to the sample sintered at 1250 ^{o}C. Simultaneously, the Ni-O band at ~ 500 cm^{-1} has lower intensity in the sample sintered at 1250 ^{o}C in comparison to the sample sintered at 1425 ^{o}C.

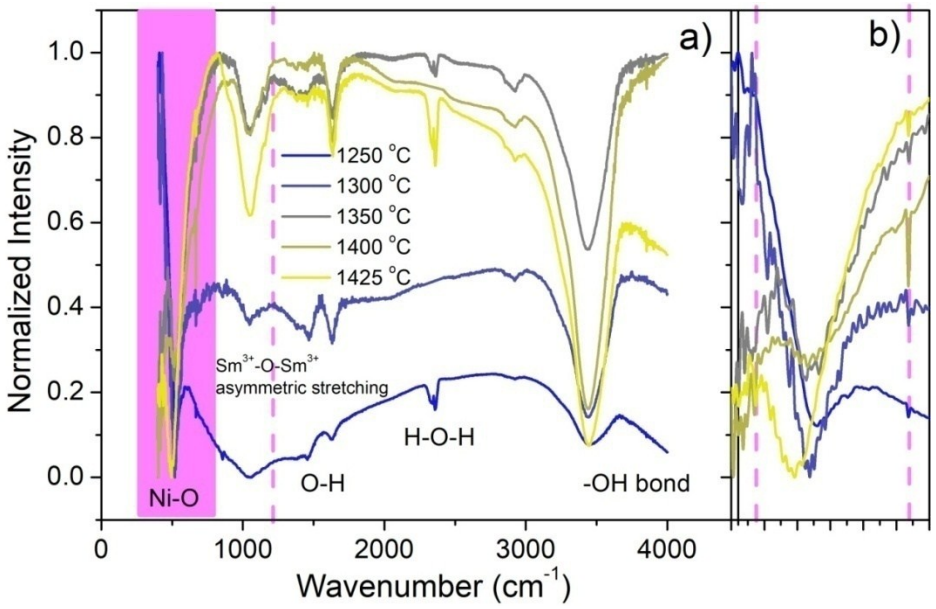

Figure S7(a) The different oxides band formations, hydroxyl band groups, are studied through FTIR transmission spectra of (SmSr)$NiO_{4-\delta}$ sample sintered at different sintering temperatures (b) FTIR spectra in the range of 400 -700 cm^{-1} for (SmSr)$NiO_{4-\delta}$ sample sintered at different sintering temperatures.

S4 Post Cyclic Voltammetry Effect

The post cyclic voltammetry effect on lattice parameters, atomic positions and occupancies for both samples 1250 °C and 1425 °C are shown in table S2.

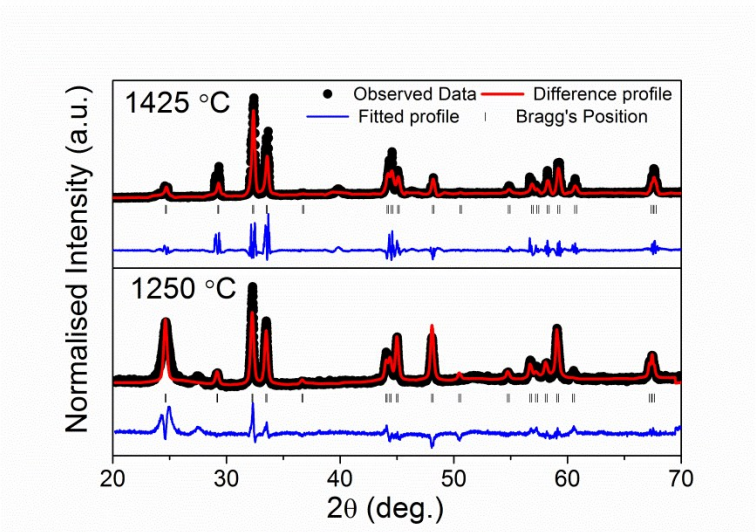

Fig.S8 Rietveld refined X-ray diffractograms of the (SmSr)$NiO_{4-\delta}$ sample sintered at 1250 °C and 1425 °C after cyclic voltammetry.

Table S2 Lattice Parameters, atomic positions and Occupancies of (SmSr)$NiO_{4-\delta}$composition after Cyclic Voltammetry

Sample	Atoms	Position				R-factor		Lattice Parameters (Å)
		x	y	z	Occupancy	Bragg R-factor	R_f factor	
1250 °C	Sm	0	0	0.3617(4)	1.26496	25	14.6	a = b= 3.784172
	Sr	0	0	0.3617(4)	1.05761			c=12.243389
	Ni	0	0	0	1.31082			
	O1	0	0.5	0	1.00000			
	O2	0	0	0.1757(7)	1.31416			
1425 °C	Sm	0	0	0.3621(8)	0.95570	12.4	7.24	a= b=3.778699
	Sr	0	0	0.3621(8)	1.05481			c=12.208506
	Ni	0	0	0	1.27142			
	O1	0	0.5	0	1.00215			
	O2	0	0	0.1592(2)	1.04720			